DEVELOPMENT AND OPTIMIZATION OF NOVEL ENCAPSULATION STRUCTURES OF INTEREST IN FUNCTIONAL FOODS THROUGH ELECTROSPRAYING

Rocio Pérez-Masiá, Jose M. Lagaron, Amparo López-Rubio*

Novel Materials and Nanotechnology Group, Institute of Agrochemistry and Food Technology (IATA-CSIC), Avda. Agustin Escardino 7, 46980 Paterna (Valencia), Spain

*Corresponding author: Tel.: +34 963900022; fax: +34 963636301.

E-mail address: amparo.lopez@iata.csic.es (A. Lopez-Rubio)

Novel Materials and Nanotechnology Group, Institute of Agrochemistry and Food Technology (IATA-CSIC), Avda. Agustin Escardino 7, 46980 Paterna (Valencia), Spain

Other e-mail addresses: rocio.perez@iata.csic.es (R. Pérez-Masiá)
lagaron@iata.csic.es (J.M. Lagaron)

Acknowledgements

A. Lopez-Rubio is recipient of a Ramon y Cajal contract from the Spanish Ministry of Science and Innovation. The authors thank the Spanish MINECO projects AGL2012-30647, FUN-C-FOOD (CSD2007-00063), and the EU project of the FP7 FRISBEE for financial support. Authors would also like to acknowledge the Central Services for Experimental Investigation Supporting (SCSIE) of the University of Valencia for the electronic microscopy service.

Abstract

The aim of this work was to establish strategies for the development of electrosprayed encapsulation structures, of interest in food applications, based on aqueous hydrocolloid dispersions. Specifically, various polysaccharides and two different proteins were evaluated for capsules formation. To this aim, the hydrocolloid dispersion properties were analysed and compared with the solution properties of two polymers readily spinnable in water (PVOH and PEO). Increasing the hydrocolloid concentration to promote chain entanglements resulted in a valid strategy only for a few matrices (related to their greater Mw). As alternative strategies to improve the physical properties and, thus, the sprayability of the dispersions, addition of gums and surfactants to modify their viscosity and surface tension, respectively, was evaluated. Moreover, denaturation of proteins was also carried out in order to investigate the effect of this treatment on the electrospraying process and on capsules formation. Results showed that the incorporation of some of these molecules, as well as protein denaturation, significantly changed the physical properties, allowing the development of encapsulation structures from all the hydrocolloids assayed. The morphology of the structures obtained was characterized and the molecular organization of some of the capsules was studied and related to the electrosprayability and capsules morphology.

Keywords: electrospinning, electrospraying, encapsulation, hydrocolloids, bioactives

1. Introduction

The encapsulation of food and nutraceutical ingredients is an emerging area of interest due to the instability of some of these compounds at ambient and digestive conditions (Ezhilarasi et al. 2013). In general, encapsulation seeks to protect these products and, thus, assure their health-promoting properties, although it can also be used to improve sensorial properties of food products containing ingredients that inherently have undesirable flavours and/or odours (Nasirullah et al. 2011).

Apart from the conventional microencapsulation techniques, such as spray drying or coarcervation, electrohydrodynamic processes have been recently suggested to be simple and straightforward methods to generate submicron encapsulation structures for a variety of bioactive molecules (Xie et al. 2008; Lopez-Rubio and Lagaron 2012; Bock et al. 2012; Pérez-Masiá et al. 2013, Bakhshi et al. 2013). These techniques use electrostatic forces to produce electrically charged jets from viscoelastic polymer solutions which on drying, by the evaporation of the solvent, produce ultrathin structures (Li and Xia 2004). When ultrathin continuous fibres are obtained, the process is called “electrospinning”. When size-reduced capsules are attained, the process is normally referred to as “electrospraying” due to the non-continuous nature of the structures obtained. For food and nutraceutical applications, capsules are generally preferred, since apart from facilitating handling and subsequent incorporation into different products, they also present greater surface/volume ratio and, thus, are expected to have better release profiles than fibres (Hong et al. 2008). The morphology and composition of micro/nanostructures attained can be modulated through controlling the process parameters, mainly the operational conditions (the high voltage applied, the distance between the spinneret and the collector and the feeding rate), the solution properties (the viscosity, the surface tension and the electrical conductivity), and the material of choice. Specifically, for food and nutraceutical applications, the encapsulating material should be suitable for human consumption. Moreover, although during the electrospraying process the solvent should be

completely evaporated, it may be convenient to only make use of allowed food contact solvents in order to avoid toxicity problems, as it has been proven that a certain amount of solvent can remain in the electrospun structures (Aceituno-Medina et al. 2013).

Electrospraying from aqueous solutions, apart from not generating toxicity problems, has the advantage of being beneficial from an environmental point of view. However, the use of water further complicates electrospraying due to the ionization of water molecules at high voltages in an air environment, which may cause corona discharge. Besides, aqueous solutions present high surface tension values which hinder the formation of stable jets during the process. Nevertheless, it is possible to obtain micro- and nanocapsules through electrospraying from aqueous solutions using some biopolymers such as polyvinyl alcohol (PVOH) or polyethylene oxide (PEO). These biopolymers have been already used for capsules formation through electrohydrodynamic processes, mainly for pharmaceutical and medical applications (Sridhar et al. 2011; Zamani et al. 2013). However, for the incorporation of the micro/nanocapsules within food matrices, the use of food hydrocolloids as encapsulating matrices is highly preferred, not only for achieving a better integration of the capsules in the foodstuffs, but also to improve assimilation of the capsules from the consumers. The use of food hydrocolloids further complicates the electrospraying process, since these materials are usually low molecular weight polymers which do not generate sufficient viscosity and that generally have strong inter- and intramolecular forces, which need to be somehow counteracted to promote capsule formation (Nagarajan et al. 2007; Stijnman et al. 2011).

In this work, a thorough study about the electrospraying of different food hydrocolloids from aqueous solutions has been carried out. Specifically, various polysaccharides, such as dextran, maltodextrin, a resistant starch, pullulan and fructooligosaccharides (FOS), and two proteins (a whey protein concentrate from milk and a soy protein isolate) were evaluated as matrix materials. To this aim, different hydrocolloid aqueous solutions were prepared, characterized and compared with the physical properties of aqueous solutions made from spinnable polymers

in water (specifically, PVOH and PEO). Specifically, the viscosity, surface tension and electrical conductivity of the solutions were evaluated. Afterwards, the physical properties of the solutions were optimized for the electrospraying process through the incorporation of different substances. Particularly, the influence of gums on the solution viscosity and the effect of surfactant addition on the surface tension values were studied when capsules could not be attained from the neat hydrocolloidal solutions. Moreover, denaturation of the proteins was also carried out in order to understand how this change in molecular conformation affected capsules formation. The morphology of the structures attained was analysed through scanning electron microscopy (SEM) and the molecular organization of the capsules was studied through attenuated total reflectance infrared spectroscopy (ATR-FTIR).

2. Materials and methods

2.1. Materials

PVOH was kindly donated by Plásticos Hidrosolubles (Spain). The commercial resistant starch was Fibersol® (www.fibersol.com) commercial grade, manufactured by ADM/Matsutani (Iowa, USA). The fructooligosaccharides (FOS) used were Fibruline Instant (FI) and Fibrulose F97, which were kindly donated by InnovaFood S.L (Spain). Whey protein concentrate (WPC) was kindly donated by ARLA (ARLA Food Ingredients, Viby, Denmark). Under the commercial name Lacprodan® DI-8090, the composition per 100 g of product consisted of ~80 g of protein, ~9 g of lactose, and ~8 g of lipids, the rest being water and minerals like sodium and potassium. Soy protein isolate (SPI) was donated by The Solae Company (Switzerland). Guar gum was purchased at Capers Community Markets (Canada). PEO, dextran, maltodextrin (DE 16.5-19.5), pullulan, Xanthan gum, Span-20 and folic acid were supplied by Sigma-Aldrich (Spain) and they were used as received, without further purification.

2.2. Preparation of the hydrocolloid dispersions

The biopolymers (PVOH and PEO) and the SPI dispersions were prepared by dissolving 5, 10 or 20% (w/v) of the polymers in distilled water. When higher concentrations of these materials were used, very dense dispersions were obtained, which were difficult to characterize. The rest of the food hydrocolloid dispersions (dextran, resistant starch, FOS, maltodextrin, pullulan and WPC) were prepared by dissolving 10, 20 or 40% (w/v) of the hydrocolloids in distilled water. 1% (w/w) of gums and/or 5% (w/w) of surfactant respect to the polymer weight were added when needed.

2.3. Characterization of the dispersions

The apparent viscosity (ηa) of the polymeric dispersions at 100 s^{-1} was determined using a rotational viscosity meter Visco Basic Plus L from Fungilab S.A. (San Feliu de Llobregat, Spain) using the Low Viscosity Adapter (LCP) spindle. The surface tension of the dispersions was measured using the Wilhemy plate method in an EasyDyne K20 tensiometer (Krüss GmbH, Hamburg, Germany). The conductivity of the dispersions was measured using a conductivity meter XS Con6 (Labbox, Barcelona, Spain). All measurements were made in triplicate at 25ºC.

2.4. Electrospraying process

The electrospraying apparatus, equipped with a variable high-voltage 0-30 kV power supply, was a Fluidnatek® basic setup assembled and supplied by BioInicia S.L. (Valencia, Spain). Details about the basic electrospraying setup can be found elsewhere (Torres-Giner et al. 2010).Dispersions were introduced in a 5 mL plastic syringe and were electrosprayed under a steady flow-rate using a stainless-steel needle with internal diameter 0.9 mm. The needle was connected through a PTFE wire to the syringe. The syringe was lying on a digitally controlled syringe pump while the needle was in horizontal towards a stainless-steel plate attached to a copper grid used as collector. The experiment was carried out at ambient conditions (20ºC and

40% RH). The conditions for obtaining the capsules were modified depending on the polymer used. Basically, the flow rate was set from 0.1 to 0.15 mL/h. Specifically, the flow rate was set at 0.1 mL/h for FOS dispersions and 0.15 mL/h for the rest of the hydrocolloid dispersions. The voltage varied from 9 to 16 kV and the distance between the tip and the collector varied from 9 to 20 cm.

2.5. Scanning electron microscopy (SEM)

SEM was conducted on a Hitachi microscope (Hitachi S-4100) at an accelerating voltage of 10 KV and a working distance of 12-16 mm. The capsules were sputtered with a gold-palladium mixture under vacuum before their morphology was examined using SEM. Capsule diameters were measured by means of the Adobe Photoshop CS3 extended software from the SEM micrographs in their original magnification.

2.6. Attenuated total reflectance infrared spectroscopy (ATR-FTIR)

ATR-FTIR spectra were collected at 25ºC in a FTIR Tensor 37 equipment (Bruker, Germany). The spectra were collected in the different materials by averaging 20 scans at 4 cm^{-1} resolution. The experiments were repeated twice to verify that the spectra were consistent between individual samples.

2.7. Statistical analysis

Statistical analysis of data was performed through analysis of variance (ANOVA) using Statgraphics Centurion XV (Manugistics Corp., Rockville, MD). Homogeneous sample groups were obtained by using LSD test (95% significant level).

3. Results and Discussion

3.1. Characterization and comparison between PVOH and PEO vs. food hydrocolloids dispersion properties and evaluation of their electrosprayability

The success of the electrohydrodynamic process strongly depends on the dispersion properties. Thus, the physical properties of the PVOH and PEO polymers and food hydrocolloidal dispersions were analysed and related to their electrospinnability/electrosprayability. The morphology of the structures obtained was also investigated. Table 1 shows the viscosity, the surface tension, the electrical conductivity and the electrospinnability of the different dispersions prepared. This table also shows the capsule's morphology and the capsule's average size in the cases where it was possible to electrospun/electrospray the dispersions. Generally, it was observed that the solutions containing the high molecular weight polymers (PVOH and PEO) had higher viscosities and lower surface tension values than the hydrocolloid-based dispersions and both conditions favoured the electrospinning process. These physical properties made that either capsules or fibres were attained from the different polymer solutions assayed. Regarding the aqueous hydrocolloidal dispersions, it was seen that only a few of them had the capacity of forming encapsulation structures through electrospraying. Specifically, only the hydrocolloids which presented a higher molecular weight and, thus, led to a significant viscosity increase when increasing the hydrocolloid concentration in the dispersion, were able to form capsules. These results can be explained on the basis of dispersion properties in relation with the electrospinning/electrospraying process. On one hand, it is well-known that electrospinning/electrospraying is only achieved when the dispersion viscosity is high enough to produce the necessary polymer entanglements to form the fibres/capsules. On the other hand, the surface tension is also a crucial parameter for the process, since high surface tension values could overcome the electrostatic forces generated by the high voltage applied and the electrical conductivity of the dispersion and, thus, hinder the Taylor cone formation and the subsequent electrospinning/electrospraying process (Bock et al. 2012; Fong et al. 1999). Regarding the

electrical conductivity, it was seen that this parameter did not considerably affect the process and, for similar viscosity and surface tension values, electrosprayability was not modified at different conductivity values. Nevertheless, it is worth noting that, if electrical conductivity is too high, there is too much charge carried by the electrospraying jet, fact that can destabilize the jet and complicate the process (Bock et al. 2012; Ding et al. 2005).

Regarding the capsules morphology it was seen that for PVOH and PEO at low polymer concentrations, beads were formed, while increasing the polymer concentration and, thus, the viscosity, fibres were obtained. This can be explained by an increase in the polymer chain entanglements when the viscosity was higher, which led to the formation of fibres. It is important to note that the chain entanglements also depend on the molecular weight of the polymers and, as a result, for similar viscosity values, different morphologies can be attained depending on the polymer used (Bock et al. 2012). Concerning the size of the structures developed, it was observed that a greater size distribution was obtained for the hydrocolloid-based capsules. This fact was probably due to the more unfavourable physical properties of these dispersions, which destabilized the electrospraying jet and led to more heterogeneous structures.

Therefore, from Table 1 it was concluded that in order to carry out a stable electrospraying process, it was necessary to modify the viscosity and the surface tension of the food hydrocolloid dispersions. Specifically, higher viscosities and lower surface tension values should be attained. Nevertheless, an exception was observed for the SPI dispersion. In this case, it was seen that although its physical properties seemed to be appropriate for capsule development through electrospraying, unstable jetting occurred and encapsulation structures could not be developed from the SPI dispersions. This fact could be related to the globular structure of the soy protein, with strong inter- and intramolecular forces which impeded chain entanglements between adjacent molecules needed for capsules formation (Vega-Lugo and Lim 2008). Therefore, protein thermal denaturation could improve the electrospraying process of SPI

dispersions since unfolding the protein chains could favour the formation of polymer entanglements.

INSERT TABLE 1 ABOUT HERE

3.2. Improvement of aqueous hydrocolloidal dispersions for electrospraying

From Table 1 it can be seen that most of the aqueous hydrocolloidal dispersions were not suitable for electrospraying and, thus, it was not possible to develop encapsulation structures from them at the various concentrations assayed. In contrast, the different PVOH and PEO solutions and some hydrocolloid-based dispersions obtained from the higher molecular weight materials (dextran, pullulan and WPC) were spinnable giving raise to either capsules or fibres depending on the solution properties. As it was commented before, the main reasons of the sprayability differences were the low viscosity together with too high surface tension values that presented most of the hydrocolloid dispersions. Various strategies were established in order to improve these physical properties and, thus, be able to electrospray the hydrocolloid-based dispersions which could not form capsules with the previous conditions assayed. For increasing the viscosity, different methodologies were followed depending on the hydrocolloid type. For the polysaccharide dispersions (resistant starch, maltodextrin, F97 and FI) some thickening agents were added. Specifically, 1% (w/w) with respect to the polymer of guar gum (GG) and xanthan gum (XG) were incorporated in the dispersions. Concerning the SPI dispersion greater viscosity values were sought by the denaturation of the protein through a thermal treatment. Denaturation leads to protein unfolding and exposure of the functional groups which could improve intermolecular interactions, both between the different protein chains and with the solvent, resulting in increased viscosity. For the reduction of the surface tension, a 5% (w/w) with respect to the polymer weight of surfactant was incorporated in both, the polysaccharide and the protein dispersions. Specifically, a non-ionic surfactant (Span-20) was

added, since it has been previously reported that electrically charged surfactants give rise to more instability in the electrospraying jet, thus, hampering capsule development (Pérez-Masiá et al. 2014). Moreover, both strategies were carried out together in order to ascertain if electrosprayability and capsule morphology were significantly affected when viscosity and surface tension were simultaneously modified. Specifically, Span-20 and guar gum were added to reduce surface tension and increase their viscosity, respectively. In the case of the SPI dispersion, the combined effect of the thermal denaturation and surfactant addition was also studied. The different strategies were investigated using the aqueous dispersions with 20% (w/v) of hydrocolloids, except for SPI, where 10% (w/v) dispersions were used. Table 2 compiles the physical properties, electrosprayability, morphology and average size of the capsules obtained from the hydrocolloid dispersions containing the different additives. From this table, it can be observed that the incorporation of the different substances effectively modified their viscosity, surface tension and conductivity, allowing stable electrospraying from almost all the hydrocolloid dispersions studied. The specific effects derived from the incorporation of the different additives on physical properties and capsule morphology are further described and discussed below.

INSERT TABLE 2 ABOUT HERE

3.2.1. Addition of gums

From Table 2 it can be observed that, as expected, the incorporation of gums to the polysaccharide dispersions significantly increased their viscosity. However, it was seen that xanthan gum led to a considerably greater increase than guar gum, due to the ability of xanthan molecules, in dispersion, to form a highly ordered network of entangled, stiff molecules through its charged trisaccharide side-chains (Norton et al. 1984). Furthermore, xanthan gum also led to greater surface tension and to a significant increase in the electrical conductivity values when

compared to guar gum, thus destabilizing the electrospraying jet. This fact explained the continuous dripping during electrospraying in all the dispersions containing xanthan gum. Another interesting observation was that, upon addition of the gums, a continuous film was formed together with the capsules in most of the materials assayed. This was probably because of the ability of gums to retain water, causing an incomplete drying of the electrospraying jet and leading to the collapse of the humid structures in the collector which formed a continuous hydrocolloid film. This effect could not be avoided even modifying the processing parameters, such as lowering the feeding rate, increasing the tip to collector distance or increasing the hydrocolloid concentration so as to facilitate the elimination of the solvent. It is also important to note that FOS also presented a greater ability to retain water than other hydrocolloids. Thus, FOS capsules were obtained by increasing the tip-to-collector distance with respect to the other hydrocolloids in order to avoid water drops on the collector. From the average capsules sizes obtained it was seen that addition of xanthan gum led to the formation of smaller structures, probably because of the higher electrical conductivity of the dispersions. Figure 1 shows the polysaccharide capsules obtained with gums. From this figure it is clearly observed that addition of xanthan gum led to the formation of smaller capsules. It was also seen that a continuous film was formed in most of the materials.

INSERT FIGURE 1 ABOUT HERE

3.2.2. SPI denaturation

As commented above, the strategy to increase the viscosity of the SPI dispersion was to apply a thermal treatment to induce denaturation, to both unfold the protein chains and expose their functional groups to facilitate entanglements. However, from Table 2, it can be observed that denaturation led to a significant viscosity decrease of the SPI dispersion. This fact could be related to the protein extraction process carried out by the suppliers. According to Vega-Lugo

and Lim (2008), as-received SPI used in this work was highly hydrolysed during the extraction process, which may have contributed to poor intermolecular interactions and thus, to its lower viscosity after the thermal treatment. Nevertheless, denaturation of SPI improved the electrospraying of this hydrocolloid, probably because of the destruction of the globular structure of the native protein, which led to greater chain entanglements. Figure 2 shows the SEM image of the SPI capsules obtained after denaturation. It was seen that multiple particles and very small capsules were obtained, probably because of the lower viscosity and the higher conductivity values of SPI. For high electrical conductivity values, the columbic repulsion forces are greater and compete with the viscoelastic forces of the dispersion, disentangling more easily the polymer network which is being formed during electrospraying. Therefore, increasing conductivity makes it easier for the dispersion to be broken up into smaller droplets, giving rise to different morphologies (Bock et al. 2012).

INSERT FIGURE 2 ABOUT HERE

3.2.3. Addition of surfactant

From Table 2 it can be observed that the incorporation of Span-20 effectively significantly dropped the surface tension of all the dispersions assayed. It was seen that for all the hydrocolloids, similar surface tension values were attained when adding the surfactant, regardless the presence or absence of gum. This fact was due to the surfactant concentration added. It is well-known that surfactants absorb at solution surfaces, thereby lowering the surface tension of the medium in which they are dissolved. Furthermore, above a critical concentration, the so-called critical micelle concentration (CMC), the surface tension of the solutions reaches an equilibrium value. The CMC of Span-20 and its respective equilibrium surface tension values in various solutions were previously studied (Pérez-Masiá et al. 2014) and it was seen to be 0.1 mM. In this work, Span-20 was added above its CMC, so the plateau

surface tension was reached in all the dispersions assayed. Figure 3 shows the SEM images of the capsules obtained from the hydrocolloid/surfactant dispersions. It was seen that addition of Span-20 to the resistant starch dispersion led to the formation of very homogenous capsules. In the case of FOS, capsules aggregation and a partial collapse of the structures were observed when Span-20 was added. This fact could be due to the greater ability of water retention of FOS, which hindered the electrospraying jet drying. In fact, tip-to-collector distance had to be increased in this case with respect to the other hydrocolloids, as it was commented before. Therefore, although the collected material was apparently dried, humid structures could be reaching the collector and causing the capsules collapse. Very small capsules with multiple morphologies were attained from maltodextrin and SPI due to the higher electrical conductivity of these dispersions. It is worth noting that addition of Span-20 enabled the electrospraying of SPI, even when it was not subjected to thermal treatment. This was probably because of an interaction between the surfactant and the protein. From Table 2 it was seen that the incorporation of Span-20 produced a significant viscosity change on the SPI dispersion, which suggested an interaction between both components. This interaction probably favoured chain entanglements during the electrospraying process and led to the capsules formation.

INSERT FIGURE 3 ABOUT HERE

3.2.4. Effect of combined addition of gums, surfactant and/or denaturation

From Table 2 it can be seen that, when the strategies to improve dispersion properties for electrospraying were carried out together, their viscosity and surface tension values were brought to suitable values for capsule formation using this electrohydrodynamic process. Figure 4 shows the SEM images of the capsules obtained combining the strategies to increase the viscosity and reduce the surface tension of the hydrocolloid dispersions. It was observed that, the presence of the gum in the case of the polysaccharide dispersions, hindered solvent

evaporation and, thus, a continuous film was also generated during the electrospraying process. This fact was mainly seen in FOS, since in this case, both the gum and the surfactant may be contributing to the water retention. In the case of SPI, when the surfactant was incorporated to the denatured protein dispersion, small, wrinkled and aggregated particles were obtained probably because of its high electrical conductivity.

INSERT FIGURE 4 ABOUT HERE

3.3. Molecular organization of the capsules

ATR-FTIR experiments were carried out in order to figure out the effect of the addition of gums and surfactants and the effect of denaturation on the molecular organization of the hydrocolloid matrices and, thus, to better understand the capsules morphologies attained. Figure 5 shows the ATR-FTIR spectra of some of the hydrocolloids assayed. Initially, resistant starch and FOS-FI capsules were analysed as an example of the polysaccharide capsules behaviour when incorporating the gums and the surfactant. Moreover, SPI capsules were also studied to better understand the influence of the thermal treatment and of the surfactant incorporation on these capsules. Figures 5A and 5B show the ATR-FTIR spectra of resistant starch and FI capsules, respectively, from 1200 to 700 cm^{-1}. This region includes the most characteristic vibrational bands of the carbohydrates. From these figures it was observed that all the electrosprayed structures presented narrower and better defined bands than the pure components, which indicated that the formation of capsules led to a greater molecular order when comparing to the bulk materials. Specifically, for the resistant starch, this area shows the C-O stretching and C-OH bending vibrations at around 1148, 1072 and 1010 cm^{-1}. Further bands were also found at around 924, 850 and 766 cm^{-1} which were attributed to skeletal vibrations of the pyranose ring, specifically to C-H stretching vibration and the α(1-6) and α(1-4) glycosidic bonds (Smrčková et al. 2013; Siddiqui et al. 2014). Concerning the spectra of the FI capsules,

Figure 5B shows the C-O-C stretching vibration at ~1110 cm^{-1}, the C-OH stretching vibration at ~1018 and 990 cm^{-1}, and the C-H stretching vibration at ~930 cm^{-1} (Tewari and Malik 2007). Another remarkable observation was that the OH stretching band which appeared at around 3300 cm^{-1} arose at lower wavenumber in FI structures than in the resistant starch ones (data not shown). Moreover, this band was also moved towards lower wavenumbers when xanthan gum was added (data not shown). The lower wavenumber indicated the presence of more bonded OH groups, probably because of greater water retention of these structures (those with FOS and with xanthan gum) as it was commented before (D'Souza et al. 2008).

INSERT FIGURE 5 ABOUT HERE

Finally, the molecular organization of the SPI capsules was also studied, to better understand the electrosprayability differences and the capsules morphology in this case. Figure 5C shows the ATR-FTIR spectra of the protein materials from 1800 to 1100 cm^{-1}, where the most characteristic protein bands are found. Specifically, the amide I and amide II bands arose at around 1630 and 1530 cm^{-1} respectively. It was observed that denaturation led to a band broadening and a shift towards higher wavenumbers of both amide bands. The broadening could be related to a greater molecular disorder due to the protein unfolding. Regarding the amide bands shift, it could be due to a protein structure variation. Specifically, the amide I shift was attributed to a secondary structure variation, since during thermal treatment the hydrogen bonds stabilizing the native structure of the proteins are disrupted, causing loss of the α-helix and β-sheets structures and creating new β-sheets arrangements (Eissa et al. 2006). The amide II band variations were related to in plane N-H and C-N vibrations (Kong and Yu 2007). Nevertheless, these changes may have favoured the protein entanglements during electrospraying and, thus, enable capsules formation.

4. Conclusions

From this study it has been demonstrated that the addition of gums and surfactants effectively modified the aqueous hydrocolloid dispersions properties allowing capsule formation through electrospraying. Results showed that, generally, addition of surfactants, and especially non-ionic surfactants, was the most interesting strategy for improving the sprayability of these materials, since gums retained too much solvent and protein denaturation led to aggregated and wrinkled particles. These results are very interesting for food-related applications, since addition of gums and surfactants allowed structure formation through electrospraying avoiding the use of organic solvents, which are not allowed in the food industry. Moreover, the use food hydrocolloids as matrix materials also favour the application of these capsules in foodstuffs. Particularly, these capsules could be used to protect different bioactive ingredients, such as vitamins, antioxidants, enzymes or probiotics, which are extremely sensitive to ambient and food processing conditions. Nevertheless, it is worth noting that matrix materials are water dispersible and, thus, their protective ability should be evaluated when incorporated to aqueous food products.

References

Aceituno-Medina, M., Lopez-Rubio, A., Mendoza, S., Lagaron, J.M. (2013). Development of novel ultrathin structures based in amaranth (*Amaranthus hypochondriacus*) protein isolate through electrospinning. Food Hydrocolloids 31, 289-298.

Bakhshi, P.K., Nangrejo, M.R., Stride, E., Edirisinghe, M. (2013). Application of electrohydrodynamic technology for folic acid encapsulation. Food and Bioprocess Technology 6 (7), pp. 1837-1846.

Bock, N., Dargaville, T.R. & Woodruff, M.A. (2012). Electrospraying of polymers with therapeutic molecules: State of the art. Progress in Polymer Science 37, 1510-1551.

Ding, L., Lee, T., Wang, C.-H. (2005). Fabrication of monodispersed Taxol-loaded particles using electrohydrodynamic atomization. Journal of Controlled Release 102 (2), pp. 395-413.

D'Souza, L., Devi, P., Divya Shridhar, M.P., Naik, C.G. (2008). Use of Fourier Transform Infrared (FTIR) spectroscopy to study cadmium-induced changes in Padina tetrastromatica (Hauck). Analytical Chemistry Insights 2008 (3), pp. 135-143

Eissa, A.S., Puhl, C., Kadla, J.F., Khan, S.A. (2006). Enzymatic cross-linking of β-lactoglobulin: Conformational properties using FTIR spectroscopy. Biomacromolecules 7 (6) , pp. 1707-1713

Ezhilarasi, P.N., Karthik, P., Chhanwal, N., Anandharamakrishnan, C. (2013). Nanoencapsulation techniques for food bioactive components: a review. Food and Bioprocess Technology 6(3), pp. 628-647.

Fong, H., Chun, I., Reneker, D.H. (1999). Beaded nanofibers formed during electrospinning. Polymer 40 (16), pp. 4585-4592.

Hong YL, Li YY, Yin YZ, Li DM, Zou GT. (2008). Electrohydrodynamic atomization of quasi-monodisperse drug-loaded spherical/wrinkled microparticles. Journal of Aerosol Science 39 (6), pp. 525-536.

Kong, J., Yu, S. (2007). Fourier transform infrared spectroscopic analysis of protein secondary structures. Acta Biochimica et Biophysica Sinica 39 (8), pp. 549-559

Li, D. & Xia, Y. (2004). Electrospinning of nanofibers: Reinventing the wheel? Advanced Materials, 16(14), 1151-1170.

Lopez-Rubio, A. & Lagaron, J.M. (2012). Whey protein capsules obtained through electrospraying for the encapsulation of bioactives. Innovative Food Science and Emerging Technologies 13, 200-206.

Nagarajan, R., Drew, C., & Mello, C.M. (2007). Polymer-micelle complex as an aid to electrospinning nanofibers from aqueous solutions. The Journal of Physical Chemistry C 111, 16105-16108.

Nasirullah, Pravin Kumar, Rizwan Shariff, (2011). Development of nutraceutical carriers for functional food applications. Nutrition & Food Science, Vol. 41 Iss: 1, pp.34 – 43.

Norton, I.T., Goodall, D.M., Frangou, S.A., Morris, E.R., Rees, D.A. (1984). Mechanism and dynamics of conformational ordering in xanthan polysaccharide. Journal of Molecular Biology 175, 371-394.

Pérez-Masiá, R., Fabra, M.J., Lagaron, J.M., López-Rubio, A. (2013). Use of electrospinning for encapsulation. In Mittal, V (Editor), *Encapsulation Technologies*. (pp. 107-136). Chemical Engineering Department, The Petroleum Institute, Abu Dhabi, United Arab Emirates.

Pérez-Masiá, R., Lagarón, J.M., López-Rubio. (2014). A Surfactant-aided electrospraying of low molecular weight carbohydrate polymers from aqueous solutions. Carbohydrate polymers (2014), 101, pp. 249-255.

Siddiqui, N.N., Aman, A., Silipo, A., Qader, S.A.U., Molinaro, A. (2014). Structural analysis and characterization of dextran produced by wild and mutant strains of *Leuconostoc mesenteroides*. Carbohydrate Polymers 99 , pp. 331-338.

Smrčková, P., Horský, J., Šárka, E., Koláček, J., Netopilík, M., Walterová, Z., Kruliš, Z., (...), Hrušková, K. (2013). Hydrolysis of wheat B-starch and characterisation of acetylated maltodextrin. Carbohydrate Polymers 98 (1) , pp. 43-49

Sridhar, R., Venugopal, J.R., Sundarrajan, S., Ravichandran, R., Ramalingam, B., Ramakrishna, S. (2011). Electrospun nanofibers for pharmaceutical and medical applications. Journal of Drug Delivery Science and Technology 21 (6), pp. 451-468.

Stijnman, A.C., Bodnar, I. & Hans Tromp, R. (2011). Electrospinning of food-grade polysaccharides. Food Hydrocolloids 25, 1393-1398.

Tewari, J.C., Malik, K. (2007). In situ laboratory analysis of sucrose in sugarcane bagasse using attenuated total reflectance spectroscopy and chemometrics. International Journal of Food Science and Technology 42 (2) , pp. 200-207.

Torres-Giner, S., Martinez-Abad, A., Ocio, M. J., & Lagaron, J. M. (2010). Stabilization of a nutraceutical omega-3 fatty acid by encapsulation in ultrathin electrosprayed zein prolamine. Journal of Food Science, 75, N69–N79.

Vega-Lugo, A.-C., Lim, L.-T. (2008). Electrospinning of soy protein isolate nanofibers. Journal of Biobased Materials and Bioenergy 2 (3), pp. 223-230

Xie, J., Li, X. & Xia, Y (2008). Putting electrospun nanofibers to work for biomedical research. Macromolecular Rapid Communications 29, 1775-1792.

Zamani, M., Prabhakaran, M.P., Ramakrishna, S. (2013). Advances in drug delivery via electrospun and electrosprayed nanomaterials. International Journal of Nanomedicine 8, pp. 2997-3017.

Table 1. Solution properties and electrosprayability of the different matrices.

Matrix (%)		Viscosity (cP)	Surface Tension (mN/m)	Electrical Conductivity (μS)	Sprayability	Morphology	Average capsule's size (μm)
PVOH (M_w ~ 100000)	5	9.1 ± 0.7[a]	40.6 ± 0.6[a]	181.3 ± 4.1[a]	YES	Capsules + thin fibers	0.7 ± 0.2[a]*
	10	28.2 ± 2.3[b]	42.1 ± 0.1[b]	300.0 ± 7.0[b]	YES	Fibers	0.1 ± 0.1[b]
	20	884.9 ± 14.1[c]	43.7 ± 0.4[c]	391.7 ± 2.1[c]	YES	Fibers	0.2 ± 0.1[b]
PEO (M_w ~ 200000)	5	58.1 ± 1.4[a]	55.9 ± 1.5[a]	144.6 ± 1.3[a]	YES	Capsules + thin fibers	0.5 ± 0.1[a]*
	10	374.1 ± 7.8[b]	53.5 ± 0.2[b]	144.4 ± 4.1[a]	YES	Capsules + thin fibers	0.5 ± 0.1[a]*
	20	18738.0 ± 106.2[c]	50.1 ± 1.8[c]	159.2 ± 2.0[b]	YES	Fibers	0.3 ± 0.1[b]
Dextran (M_w ~ 70000)	10	10.9 ± 0.5[a]	57.3 ± 0.1[a]	50.4 ± 2.3[a]	NO	---	---
	20	28.8 ± 0.1[b]	54.2 ± 0.3[b]	28.9 ± 0.8[b]	NO	---	---
	40	94.2 ± 2.9[c]	59.3 ± 0.3[c]	23.5 ± 0.5[c]	YES	Capsules	0.9 ± 0.5[a]
Resistant Starch (M_w ~ 1700-2700)	10	4.4 ± 0.5[a]	59.2 ± 0.4[a]	28.8 ± 2.2[a]	NO	---	---
	20	5.5 ± 0.5[a]	57.1 ± 1.6[b]	18.0 ± 1.1[b]	NO	---	---
	40	9.1 ± 0.9[b]	57.9 ± 0.8[ab]	18.9 ± 0.6[b]	NO	---	---
Maltodextrin (M_w ~ 1300)	10	4.8 ± 0.5[a]	52.0 ± 0.7[a]	503.0 ± 1.4[a]	NO	---	---
	20	5.2 ± 0.2[a]	52.7 ± 0.1[a]	677.5 ± 0.7[b]	NO	---	---
	40	5.3 ± 0.5[a]	51.6 ± 0.4[a]	896.7 ± 1.2[c]	NO	---	---
Pullulan (M_w ~ 100000)	10	18.9 ± 0.1[a]	58.7 ± 0.1[a]	19. 7 ± 0.5[a]	NO	---	---
	20	133.3 ± 0.7[b]	53.2 ± 0.2[b]	17.3 ± 0.4[b]	YES	Capsules + thin fibers	1.0 ± 0.7[a]*
	40	1690.6 ± 9.1[c]	58.5 ± 1.4[a]	16.8 ± 0.1[b]	YES	Fibers	0.1 ± 0.1[b]
FOS-F97 (M_w ~ 330-	10	4.8 ± 0.2[a]	61.6 ± 0.8[a]	51.1 ± 1.5[a]	NO	---	---
	20	5.2 ± 0.6[a]	63.6 ± 0.9[b]	49.9 ± 0.7[a]	NO	---	---

6500)	40	7.2 ± 1.2[b]	64.3 ± 0.1[b]	44.7 ± 0.1[b]	NO	---	---
FOS-FI (M_w ~ 330-8100)	10	5.4 ± 0.4[a]	59.9 ± 0.4[a]	72.0 ± 3.6[a]	NO	---	---
	20	5.6 ± 0.3[a]	58.6 ± 1.0[b]	69.1 ± 1.6[a]	NO	---	---
	40	8.29 ± 0.5[b]	58.1 ±0.2[b]	79.9 ± 3.1[b]	NO	---	---
WPC (M_w ~ 20000-70000)	10	5.4 ± 0.3[a]	46.7 ± 1.0[a]	1643.0 ± 25.5[a]	NO	---	---
	20	10.8 ± 0.5[b]	46.5 ± 0.7[a]	2280.0 ± 10.1[b]	YES	Multiple particles	---
	40	49.0 ± 1.3[c]	41.9 ± 0.2[b]	2753.3 ± 20.8[c]	YES	Capsules	1.0 ± 0.6[a]
SPI (M_w ~ 30000-350000)	5	10.6 ± 0.4[a]	44.4 ± 0.6[a]	1689.7 ± 11.0[a]	NO	---	---
	10	70.5 ± 3.4[b]	44.4 ± 0.5[a]	2723.3 ± 23.1[b]	NO	---	---
	20	---	---	---	NO	---	---

1

2

Table 2. Solution properties, electrosprayability and morphology of the different hydrocolloidal solutions with different additives: guar gum (GG), xanthan gum (XG) and Span-20.

Matrix (%)	Additive (%)	Viscosity (cP)	Surface Tension (mN/m)	Electrical Conductivity (μS)	Sprayability	Morphology	Average capsule's size (μm)
Resistant Starch (20%)	---	5.5 ± 0.5 [a]	57.1 ± 1.6[a]	18.0 ± 1.1[a]	NO	---	---
	GG (1%)	11.6 ± 0.3 [b]	55.3 ± 0.6[b]	24.3 ± 0.2[b]	YES	Capsules + Films	0.8 ± 0.6[a]
	XG (1%)	177.7 ± 0.6[c]	58.5 ± 0.3[c]	147.5 ± 1.0[c]	YES	Capsules + Films	0.4 ± 0.3[b]
	Span-20 (5%)	5.6 ± 0.3 [a]	25.6 ± 0.1[d]	25.3 ± 0.5[bd]	YES	Capsules	0.5 ± 0.4[b]
	GG (1%)/Span-20 (5%)	11.4 ± 0.3 [b]	25.9 ± 0.1[d]	26.7 ± 1.7[d]	YES	Beads + Films	0.7 ± 0.3[a]
Maltodextrin (20%)	---	5.2 ± 0.2 [a]	52.7 ± 0.1[a]	677.5 ± 0.7[a]	NO	---	---
	GG (1%)	11.2 ± 0.2 [b]	50.0 ± 0.5[b]	697.0 ± 4.6[b]	YES	Capsules + Films	0.7 ± 0.6[a]
	XG (1%)	58.6 ± 0.8[c]	50.1 ± 2.1[b]	822.0 ± 12.2[c]	YES	Capsules + Films	0.3 ± 0.2[b]
	Span-20 (5%)	5.8 ± 0.1 [a]	25.1 ± 0.6[c]	681.0 ± 7.1[a]	YES	Capsules	0.1 ± 0.1[c]
	GG (1%)+ Span-20 (5%)	11.6 ± 0.3 [b]	25.4 ± 0.2[c]	694.3 ± 5.3[b]	YES	Capsules + Films	0.6 ± 0.5[a]
FOS-F97 (20%)	---	5.2 ± 0.6 [a]	63.6 ± 0.9[a]	49.9 ± 0.7[a]	NO	---	---
	GG (1%)	16.9 ± 0.8 [b]	39.1 ± 0.8[b]	47.9 ± 0.6[a]	YES	Capsules + Films	0.6 ± 0.8[a]
	XG (1%)	192.0 ± 5.2[c]	48.4 ± 0.2[c]	168.4 ± 2.2[b]	YES	Capsules + Films	0.3 ± 0.5[b]
	Span-20 (5%)	5.3 ± 0.3 [a]	26.0 ± 0.6[d]	55.1 ± 0.4[c]	YES	Capsules (Aggregates)	0.6 ± 0.3[a]
	GG (1%)+ Span-20 (5%)	16.5 ± 1.1 [b]	25.8 ± 0.2[d]	71.1 ± 1.8[d]	YES	Capsules + Films	1.7 ± 1.2[c]
FOS-FI (20%)	---	5.6 ± 0.3 [a]	58.6 ± 1.0[a]	69.1 ± 1.6[a]	NO	---	---
	GG (1%)	18.1 ± 1.3 [b]	49.9 ± 1.7[b]	80.5 ± 3.5[b]	YES	Capsules	0.6 ± 0.8[a]
	XG (1%)	542.6 ± 10.5[c]	58.1 ± 2.0[a]	227.7 ± 2.5[c]	YES	Capsules + Films	0.1 ± 0.1[b]
	Span-20 (5%)	5.5 ± 0.2 [a]	26.0 ± 0.2[c]	62.9 ± 0.2[d]	YES	Capsules (Aggregates)	0.5 ± 0.3[a]
	GG (1%)+ Span-20	45.4 ± 2.8[d]	25.5 ± 0.1[c]	80.0 ± 1.5[b]	YES	Capsules + Films	0.3 ± 0.3[c]

	(5%)						
SPI (10%)	---	70.5 ± 3.4 [a]	44.4 ± 0.5 [a]	2723.3 ± 23.1 [a]	NO	---	---
	Denaturation	26.6 ± 4.1 [b]	42.6 ± 0.7 [b]	2810.0 ± 40.0 [b]	YES	Capsules/Particles	0.2 ± 0.1 [a]
	Span-20 (5%)	59.0 ± 0.8 [c]	32.3 ± 0.3 [c]	2643.3 ± 15.3 [c]	YES	Capsules/Particles	0.3 ± 0.2 [b]
	Denat + Span-20 (5%)	56.3 ± 2.0 [c]	32.0 ± 0.3 [c]	2493.3 ± 35.1 [d]	YES	Capsules/Particles	0.2 ± 0.1 [c]

1

FIGURE CAPTIONS

Figure 1. SEM images of capsules with 1% (w/w) of gum obtained from 20% (w/v) hydrocolloidal dispersions: (A) Resistant Starch/GG; (B) Maltodextrin/GG; (C) FOS-F97/GG; (D) FOS-FI/GG; (E) Resistant Starch/XG; (F) Maltodextrin/XG; (G) FOS-F97/XG; and (H) FOS-FI/XG. Scale marks correspond to 5 µm.

Figure 2. SEM image of capsules obtained from 10% (w/v) SPI solutions after denaturation.

Figure 3. SEM images capsules with 5% (w/w) of Span-20 obtained from different hydrocolloidal dispersions: (A) 20% (w/v) Resistant starch; (B) 20% (w/v) Maltodextrin; (C) 20% (w/v) FOS-F97; (D) 20% (w/v) FOS-FI; and (E) 10% (w/v) SPI. Scale marks correspond to 5 µm (images A, C and D) and 2 µm (images B and E).

Figure 4. SEM images of capsules with 1% (w/w) of guar gum (GG) and 5% (w/w) of Span-20 obtained from the different hydrocolloidal dispersions: (A) Resistant Starch/GG/Span-20; (B) Maltodextrin/GG/Span-20, (C) FOS-F97/GG/Span-20 and (D) FOS-FI/GG/Span-20; and (E) denatured SPI/Span20. Scale marks correspond to 5 µm.

Figure 5. ATR-FTIR spectra of electrosprayed capsules obtained from different hydrocolloidal dispersions: (A) resistant starch; (B) FOS-FI; and (C) SPI.

1

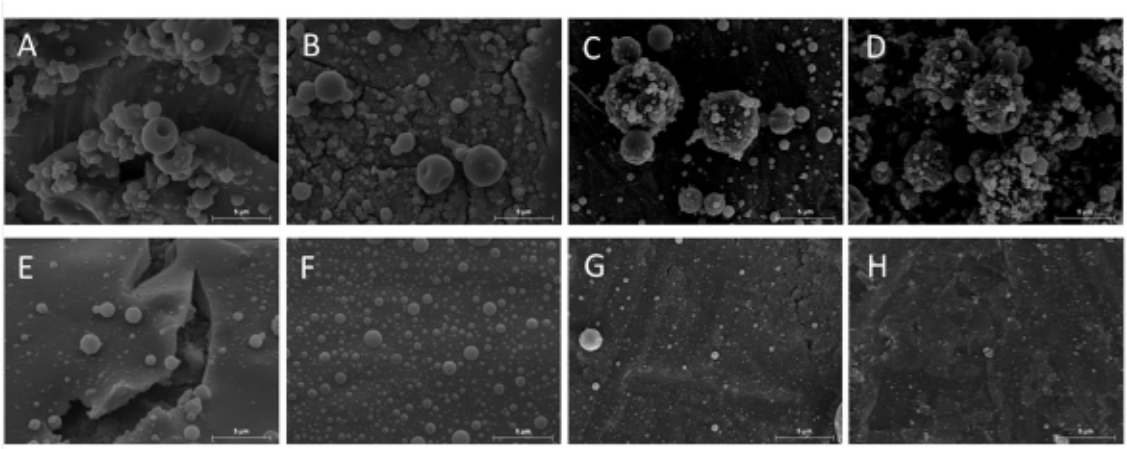

FIGURE 1.

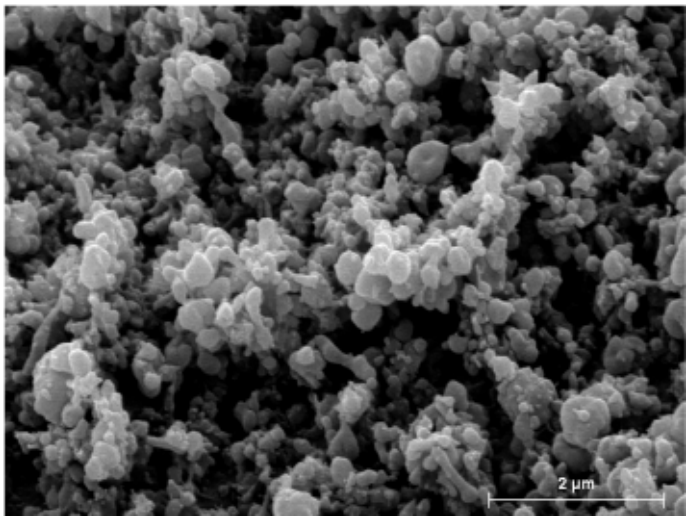

FIGURE 2.

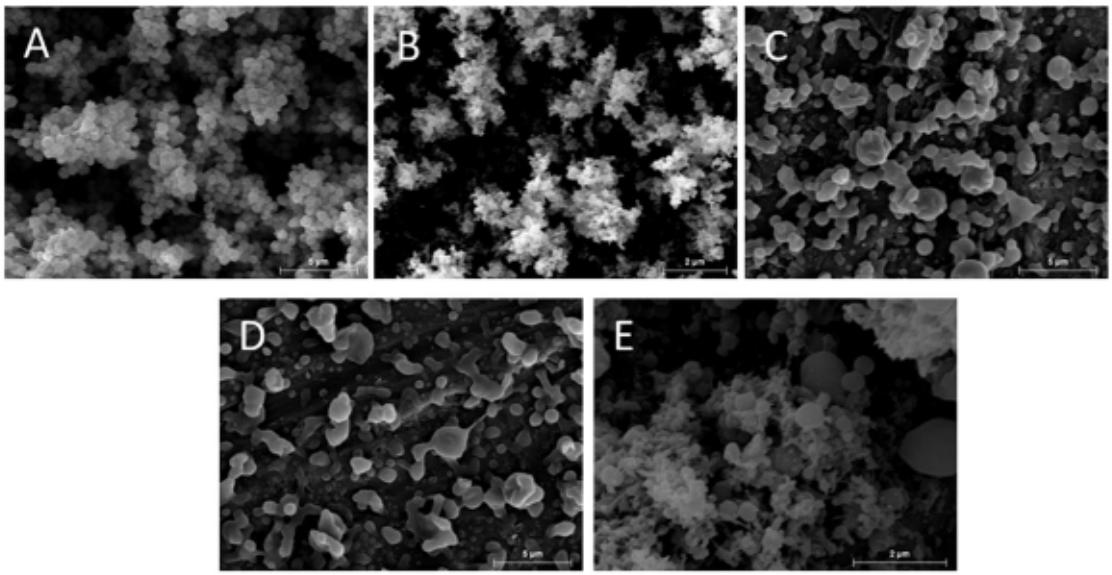

FIGURE 3.

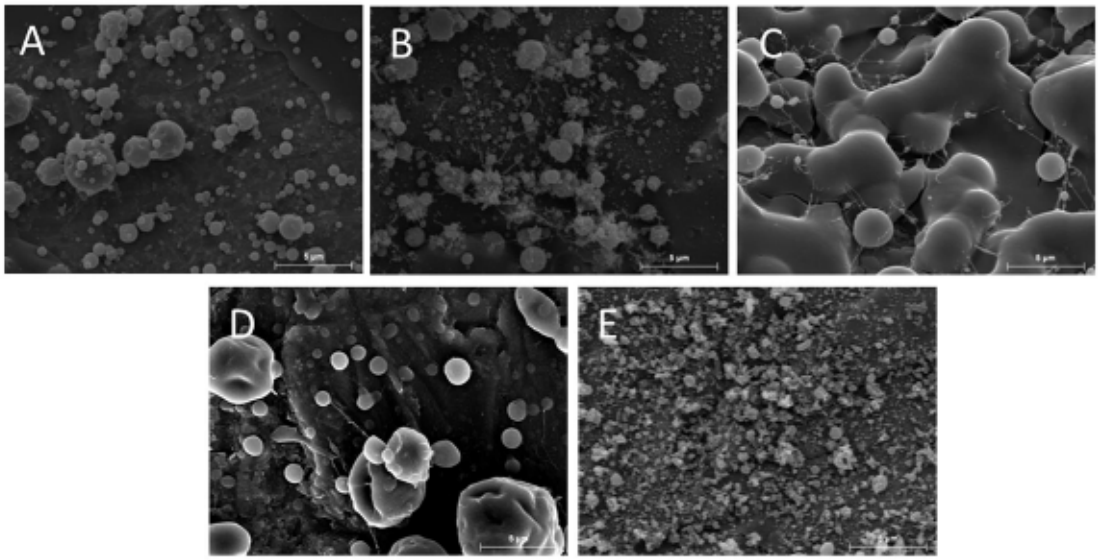

FIGURE 4.

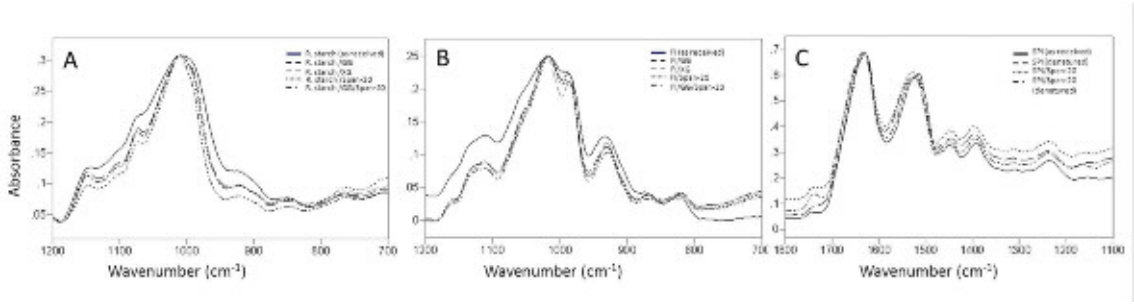
A
B
C
Absorbance
Wavenumber (cm-1)
Wavenumber (cm-1)
Wavenumber (cm-1)

FIGURE 5.